Studies on Lithium-Ion Diffusion in Heat-Treated CNBs by Microelectrode Method

Sano, Atsushi; Kurihara, Masato; Abe, Takeshi; Ogumi, Zempachi

Journal of The Electrochemical Society, **156** (8) A639-A644 (2009) A639
0013-4651/2009/156(8)/A639/6/$25.00 © The Electrochemical Society

Studies on Lithium-Ion Diffusion in Heat-Treated CNBs by Microelectrode Method

Atsushi Sano,[a,*,z] Masato Kurihara,[a,*] Takeshi Abe,[b,*] and Zempachi Ogumi[b,]**

[a]*TDK Corporation, Device Development Center, Chiba 286-8588, Japan*
[b]*Department of Energy and Hydrocarbon Chemistry, Graduate School of Engineering, Kyoto University, Kyoto 615-8510, Japan*

The ability of lithium-ion diffusion in carbon nanobeads (CNBs) was investigated by the microelectrode method [cyclic voltammetry, constant current charge/discharge, potential step, and potentiostatic intermittent titration technique (PITT)]. CNBs showed high rate discharge capacities of over 1000 C. CNB heat-treated at 1000, 1500, and 2000°C showed a higher charge ability than 2800°C. The lithium-ion diffusion coefficient (D_{Li^+}) in CNBs was investigated by PITT. D_{Li^+} was different in the intercalation and deintercalation directions in 1000, 1200, and 1500°C CNBs. D_{Li^+} of the intercalation and the deintercalation showed different potential dependencies. The 1200°C heat-treated CNB showed the highest D_{Li^+} in the direction of intercalation.
 [DOI: 10.1149/1.3138724]

Manuscript submitted February 23, 2009; revised manuscript received April 21, 2009. Published May 26, 2009.

Recently, high rate charge/discharge energy devices have attracted attention. The high rate lithium-ion battery is especially interesting for its application to the hybrid electric vehicles and power tools. This is because the lithium-ion battery has a higher voltage than other energy devices such as the electric double layer capacitor or the Ni–H battery.

Graphite or nongraphitized carbon is used for the negative electrode of the lithium-ion battery. Lithium-ion intercalates to a carbon electrode during charging and deintercalates during discharging. The speed of intercalation and deintercalation determines the input power and output power of the negative electrode. Therefore, the diffusion of lithium ion in the carbon electrode is important to the design and cell performance. The diffusion coefficient (D_{Li^+}) of lithium ion in a graphite negative electrode was investigated by potentiostatic intermittent titration (PITT), impedance spectroscopy, and cyclic voltammetry (CV).[1-5] This value of D_{Li^+} is 10^{-6}–10^{-10} cm^2 s^{-1}. Levi et al. concluded that the D_{Li^+} does not depend on the thickness of the electrode but depends on the basal plane dimension for the particles. Funabiki et al.[4,5] specified the surface area of the edge plane and basal planes by using highly oriented pyrolytic graphite. They investigated the lithium-ion diffusion and the phase boundary for different stages of graphite intercalated compounds by the method of potential step chronoamperometry (PSCA). Phase boundary movement was initially determined by the rate of reaction at the graphite/electrolyte interface and was thereafter determined by the diffusion of lithium ions in the graphite. Because small particles have shorter diffusion lengths than larger particles, small particles have an advantage in Li-ion diffusion into graphite.

Aurbach et al. reported on the diffusion coefficient of lithium ion in a graphite electrode by PITT and Warburg impedance.[1,6,7] They also investigated the dependence on the graphite particle size. Their data suggest that as the graphite size becomes smaller, the diffusion coefficient of Li ion into the graphite becomes smaller. They explained this result in terms of an edge effect of the surface films partially covering the graphite particles.

Wang et al. investigated graphitized carbon nanobeads (GCNBs). GCNBs have an onionlike texture and a diameter of about 0.2 μm.[8] By transmission electron microscope (TEM) imaging, they found that this uniquely shaped carbon does not aggregate like carbon blacks. Typical graphite cannot be used in propylene carbonate (PC) because the graphite layer exfoliates in PC-based electrolytes when the Li ion intercalates into graphite. But GCNBs showed reversible intercalation and deintercalation in PC-based electrolytes. The high rate discharge capacity was larger than mesocarbon microbeads (MCMBs). They concluded that this high rate performance was due to the short diffusion path of GCNBs and that the resistance of solid electrolyte interphase was very small.

We focused on carbon nanobeads (CNBs) for high rate charge and high rate discharge use. The electrochemical characteristics of CNB heat-treated from 1000 to 2800°C were investigated. In our investigation, we used the microelectrode method to measure CV, constant current charge/discharge, PSCA, and PITT.

Single-particle electrochemical measurement was studied by Uchida et al.[9-11] They used microsized single particles or secondary particles for CV or ac impedance measurement. In this study, we used the secondary particles of CNB, which have dimensions of around 30 μm for the secondary particle and 0.2 μm for the primary particle. The microelectrode measure has some merit. Li-ion diffusion into an electrolyte is spherical diffusion; thus the Li-ion diffusion in an electrolyte is faster than that in the usual combined electrode. In the microelectrode method, a binder or an electroconductive material is not used. Therefore it is possible to evaluate the performance of the active material itself. By using these methods, we investigated the electrochemical characteristics of heat-treated CNBs.

Experimental

CNBs were prepared by chemical vapor deposition at Tokai Carbon Co. Ltd. The details of the preparation procedure were reported previously.[8,12] The CNB were heat-treated in an electric oven under Ar atmosphere at 1200, 1500, 2000, and 2800°C. The temperature was maintained for 20 h.

Microelectrode measurement.— A schematic view of the equipment is shown in Fig. 1. The cell formation was in a two-electrode cell. Heat-treated CNBs were used as the working electrodes. A CNB was composed of aggregations of CNB particles. The diameter of the aggregation was approximately 30 μm, which was selected for the measurement. MCMBs (Osaka gas) were also used as the active material of working electrodes. Special use stainless steel wire (10 μm) covered with glass as an insulator was contacted with the working electrode for the current collection. The counter electrode was lithium metal. We determined that the Ohmic drop and the impedance of the counter electrode were low enough to evaluate the working electrode. 1 mol dm^{-3} $LiPF_6$ dissolved in ethylene carbonate:diethyl carbonate (3:7) (volume ratio) was used as the electrolyte. All electrochemical measurements were carried out in an Ar glove box (the dew point is below −70°C).

Electrochemical measurements were carried out by HZ3000 (Hokuto denko). CV, constant current charge/discharge, PSCA, and PITT were measured. CV was carried out at various sweep rates from 0.5 to 640 mV/s. In the constant current charge/discharge measurements, the current was set between 10 and 2000 nA. The cutoff

* Electrochemical Society Active Member.
** Electrochemical Society Fellow.
z E-mail: sanoa@jp.tdk.com

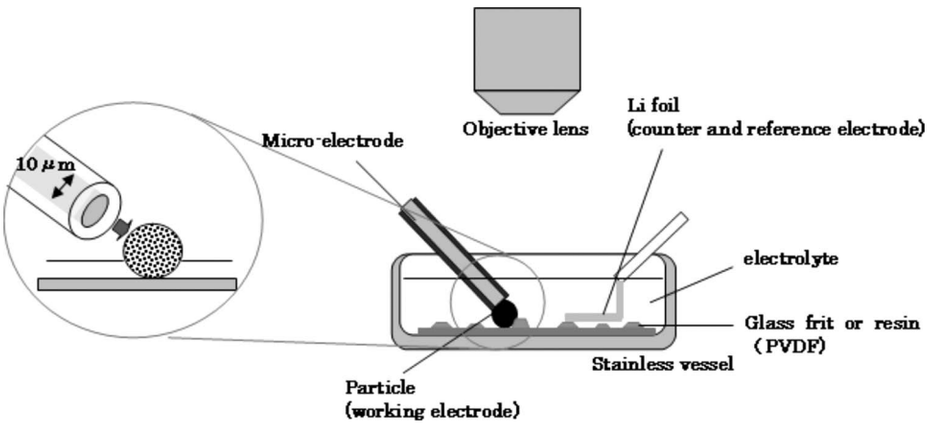

Figure 1. Schematic image of small electrode measurement equipment.

potential was 0–3.0 V vs Li/Li^+. TEM (JEM3010, JEOL) was used for the observation of the structure of CNBs. CNB samples were on a gold microgrid.

Results

The TEM images of heat-treated CNBs are shown in Fig. 2. A graphitized layer structure was not observed in the CNB heat-treated to 1000°C. The CNB heated to 1200°C showed a slight concentric ring structure. A black dot and a wave form structure were observed for the 1500°C temperature. The black dot structure means strain in the structure. Thus the 1500°C-heated CNB has a distorted layer structure in the circumferential direction. The 2000°C-heated CNB formed a specific layered structure with a polyhedron face, which is a well-developed layer structure. The 2800°C-heated CNB has more strain than the 2000°C-heated one. It seems that each basal plane was pushed together and caused the strain. The inner part of the 2800°C-heated CNB was a ribbonlike carbon. This suggests that the large strain at this heating temperature prevented the development of a graphite structure in the inner layer. The outermost layer for this 2800°C-heated CNB was coated with amorphous-like carbon.

Figure 3 shows the optical microscope images of CNBs and MCMBs used in this experiment. The MCMB used in the measurement was a single particle. The sizes of the CNB and the MCMB were selected to be close both in capacity and in dimension.

CV was carried out in the microelectrode method (Fig. 4). In 1000 and 1200°C heat-treated CNBs, cathodic current peaks were observed at 0.20 and 0 V while anodic current peaks were observed at 0.25 and 1.0 V. The cathodic peak at 0 V corresponds to the anodic peak at 0.25 V, and the cathodic peak at 0.20 V corresponds to the anodic peak at 1.0 V. These redox pairs show the lithium-ion intercalation to CNB and deintercalation.[13-16] Dahn et al.[13-15] and Tatsumi et al.[16] reported that soft carbons heat-treated at low temperatures showed redox pairs at around 1.0 V. In the 1500°C heat-treated CNB, a cathodic current peak was observed at 0.65 V and an anodic current peak was observed at 1.0 V. In the 1500°C heat-treated CNB, the hysteresis is smaller than that in 1000 and 1200°C heat-treated CNBs. In the 2000°C heat-treated CNB, one cathodic peak and one anodic peak were observed. The anodic peak was at 0.3 V. At 2800°C, the anodic peak was observed at 0.25 V. The anodic peaks of the CNBs decreased as the temperature of heat-treatment increased. The anodic peak of the MCMB was 0.42 V, which is higher than that for the 2800°C heat-treated CNB. The intercalation/deintercalation of MCMB needs a larger overpotential than CNB 2800°C. This result indicates that the lithium-ion diffusion in CNB is faster than in MCMB.

We investigated the relationship between the sweep rate (0.5–640 mV/s) and the cathodic capacities integrated by the cathodic current (Fig. 5). Heat-treatment at 1000, 1200, or 1500°C did not

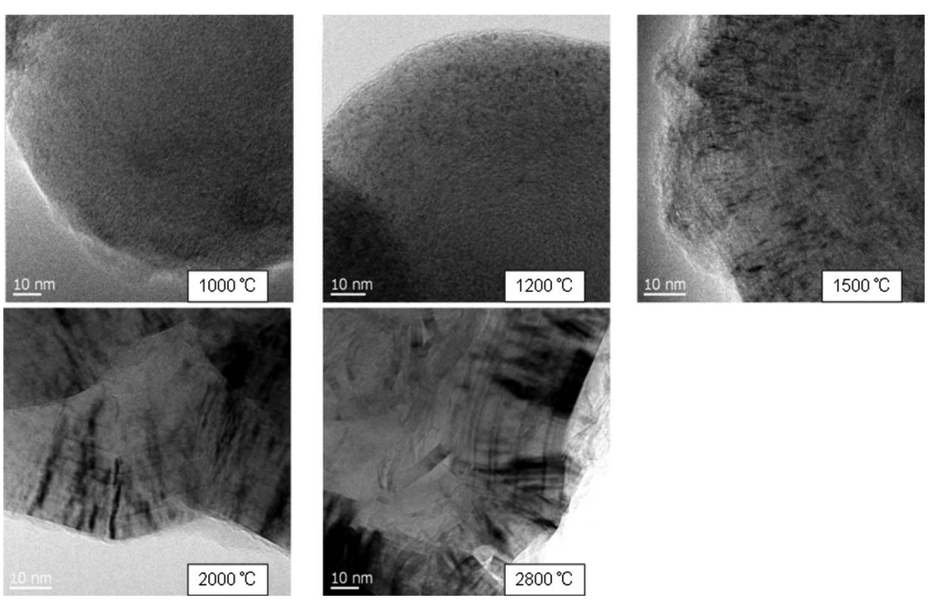

Figure 2. TEM images of heat-treated CNB.

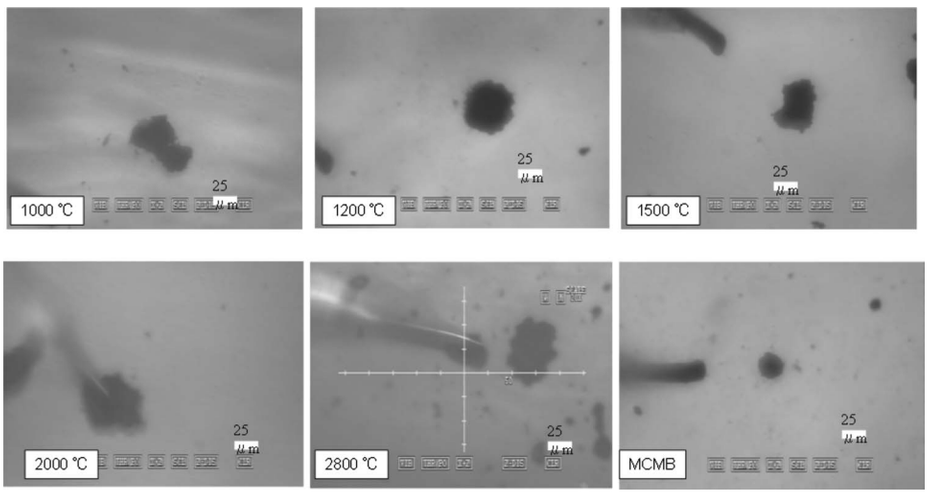

Figure 3. Optimal images of heat-treated CNB measured by small particle electrode method.

make much difference. In the 2000°C heat-treated CNB, the capacity was slightly lower than that for the CNB heat-treated below 1500°C. The capacity of the 2800°C heat-treated CNB was much lower than that for the 2000°C heat-treated CNB especially at the high rate. This is probably due to the ratio of the basal plane to the edge plane. The lithium ion intercalates from the edge plane only. The 2000°C heat-treated CNB should have more edge than the 2800°C one because the basal plane is not well developed in the 2000°C heat-treatment. More edge planes enable the rapid kinetic lithium-ion intercalation. The other mechanism that we propose is based on the structure of CNBs. The 2800°C-heated CNB contains a larger distortion in the graphene sheet than the 2000°C-heated one. This was observed by TEM. This distortion should interrupt the smooth lithium-ion intercalation.

We investigated the relationship between the sweep rate (1–640 mV/s) and the anodic capacities measured by CV. The tendency was similar to the cathodic capacities shown in Fig. 5. This result indicates that the capacity is determined by the cathodic sweep rate because the intercalation rate was slower than that of the deintercalation.

The constant current charge/discharge was carried out (Fig. 6). The 1000 and 1200°C heat-treated CNBs show moderate curves between 0 and 3.0 V. This behavior is observed in low temperature heat-treated soft carbons.[13-16] The average charge/discharge potential decreased as the temperature of the heat-treatment of the CNB increased. These behaviors are similar to the electrochemical properties of petroleum cokes heat-treated at various temperatures.[16] MCMBs showed different discharge curves compared with CNBs. MCMBs exhibit a large Ohmic drop followed by a flat potential. This result is most likely due to the difference in structure between CNBs and MCMBs.

The relationship between the discharge rate and the discharge capacity is shown in Fig. 7. All samples were able to discharge above the 1000 C rate, which means fully discharged at 1/1000 h. In the microelectrode method, lithium-ion diffusion into the electrolyte is spherical, which decreases the concentration polarization in the electrolyte and enables a rapid lithium-ion diffusion. The 1200°C heat-treated CNB showed the highest rate performance, and the 2000°C one was lowest. These results contain an Ohmic drop, an average potential, and a cutoff potential. Thus it is not easy to com-

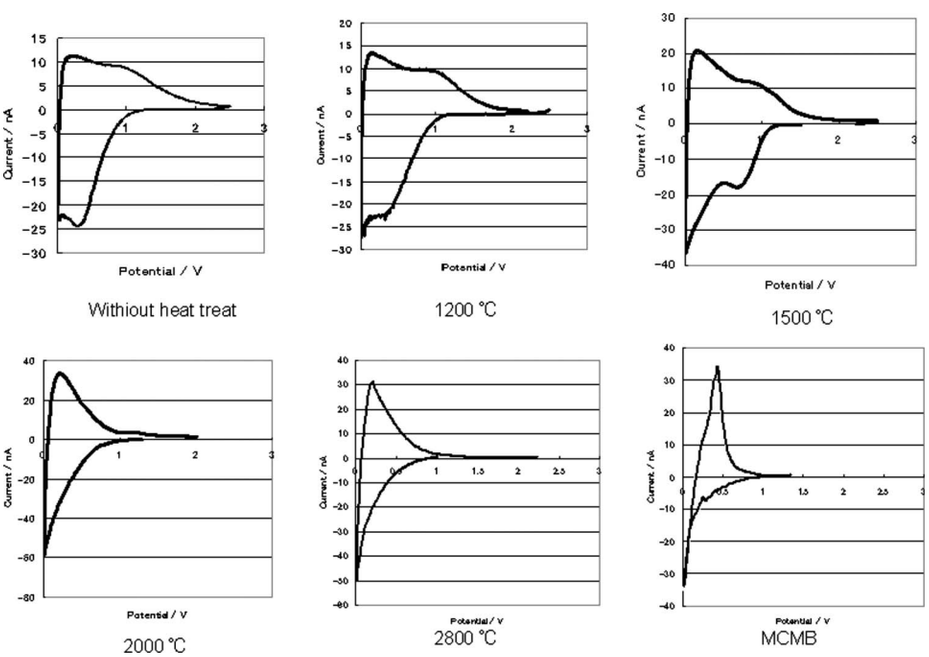

Figure 4. CV of heat-treated CNB after several cycles. Sweep rate: 5 mV/s.

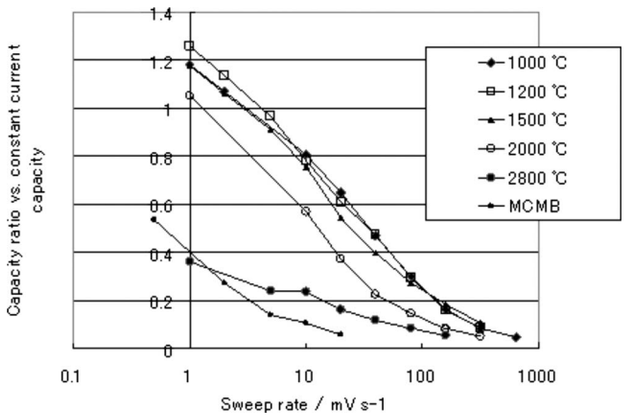

Figure 5. Relationship between sweep rate and cathodic capacity ratio vs constant current capacity

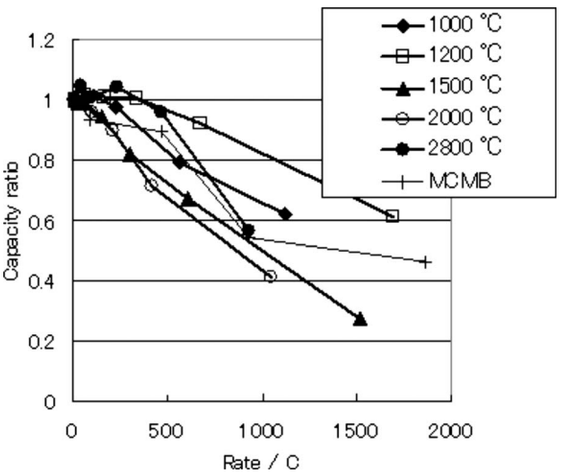

Figure 7. Ultrahigh rate discharge of heat-treated CNB.

pare the discharge rate directly. However, it is obvious that CNBs showed a high rate performance for over 1000 C discharge.

The discharge rate was measured by the potential step method (Fig. 8). The potential was stepped from 0.05 to 1.5 V. The time after the potential was stepped, and the discharge capacity was measured. The 1200°C heat-treated CNB had the fastest discharge, with the discharge rate increasing in the following order: 1000 ≒ 2000, 1500, and 2800°C heat-treated CNB and MCMB. The 1200, 1000, and 2000°C heat-treated CNBs showed similar performances. The 1500°C was slightly slower than the 1200, 1000, and 2000°C heat-treated CNB. The 2800°C CNB was significantly slower than other temperatures. The potential gap between the average deintercalation potential and the set potential (1.5 V) is an important factor because the large potential gap is advantageous for a rapid discharge. The 2800°C heat-treated CNB has the largest potential gap among the CNBs. Nevertheless, the discharge rate for this 2800°C treatment was lowest. Based on these results, the lithium-ion diffusion in the 2800°C CNB is slow, and it is due to the fewer diffusion paths observed by TEM images than for other CNBs. It is most likely attributed to the distortion of the basal plane. The discharge rate for the MCMB is much faster than that for the 2800°C heat-treated CNB. This is expected because of the lamellar structure of the MCMB.

Figure 9 shows the charge rate measured by the potential step method. The potential was stepped from the discharged open-circuit potential to 0.05 V. The time and the charge capacity were measured. The charging rate followed the temperature of heat-treatment, 1000 > 1200 > 1500 > 2000 > 2800 °C > MCMB. This result reflects the specific structure of the CNB observed in the discharge rate performance and the effect of the potential gap between the intercalation potential and the set potential (0.05 V). The lower potential gap of the higher temperature CNB leads to a lower charge rate.

The discharge rate of the MCMB was much higher than that of the 2800°C heat-treated CNB. However, the charge rate of the MCMB was much slower than that of the 2800°C heat-treated CNB. It is interesting to consider the mechanism of the high rate charge and discharge, which is attributed to the graphite structure.

The lithium-ion diffusion constant was investigated by the PITT method. Gnanaraj et al.[17] and Wen et al.[18] introduced log t and $It^{1/2}$ plots to specify the Cotterell region time. The maximum value of $It^{1/2}$ appears in the neighborhood of the characteristic diffusion time τ. The maximum value of $It^{1/2}$ moved to the left, which shows that lithium-ion diffusion is faster.

Figure 10 shows the potential dependence of the diffusion constant (D_{Li^+}). D_{Li^+} was calculated by the formula

$$\tau = (Qm\Delta X/\pi^{1/2}It^{1/2})^2$$

$$\tau = l^2/D_{Li^+}$$

where Qm is the total capacity of the intercalation or deintercalation and l is the diffusion length. Aurbach et al. assumed l as the radius of the graphite particle.[1,17] In this study, we took l as the half of the particle size of CNB (0.1 μm).

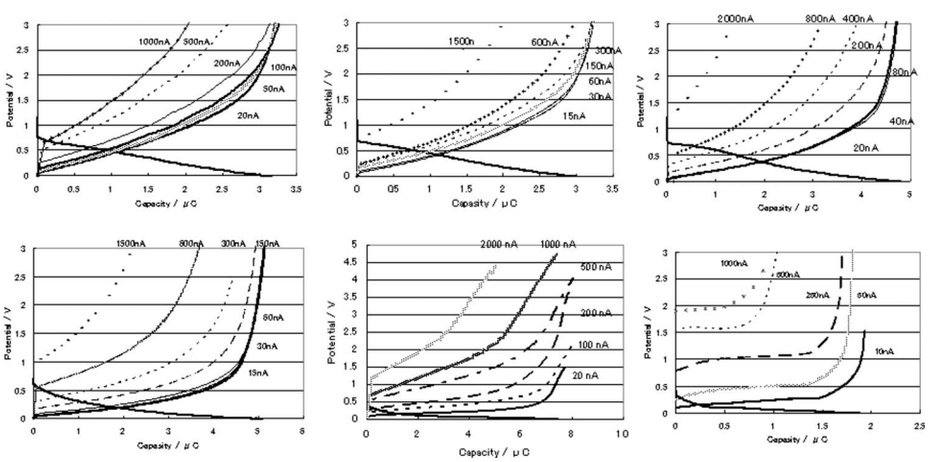

Figure 6. Charge and discharge curves of heat-treated CNB (constant current).

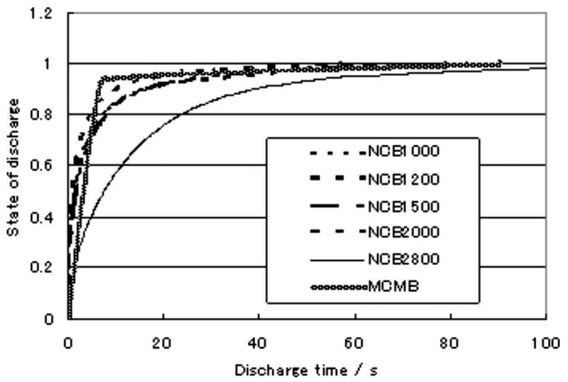

Figure 8. Relationship between potential step discharge time (from 0.05 to 1.5 V) and state of discharge.

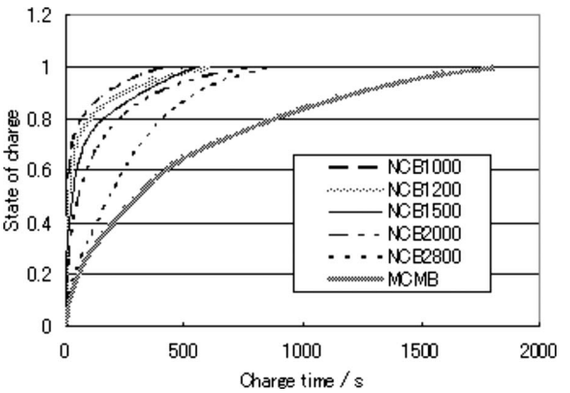

Figure 9. Relationship between potential step charge time (from open-circuit voltage to 0.05 V) and state of charge.

In the 2800°C heat-treated CNB, D_{Li^+} increased as the potential increased. D_{Li^+} was around 10^{-12}–10^{-11} cm/s. This value is lower than a reported value for graphite.[1,17] It should be taken into account that CNB consists of aggregated particles, and diffusion into the core of the aggregated particle may control the diffusion rate. In that case, the diffusion length should be assumed to be more than 0.1 μm, and D_{Li^+} would thus take on a larger value. Aurbach et al. reported that smaller particles have a smaller D_{Li^+}.[9] This result might be due to the assumption of a shorter diffusion length *l*. Dokko et al. assumed the diameter of the aggregated particle as the diffusion length *l*. In this paper, we used the radius of the CNB as the diffusion length.

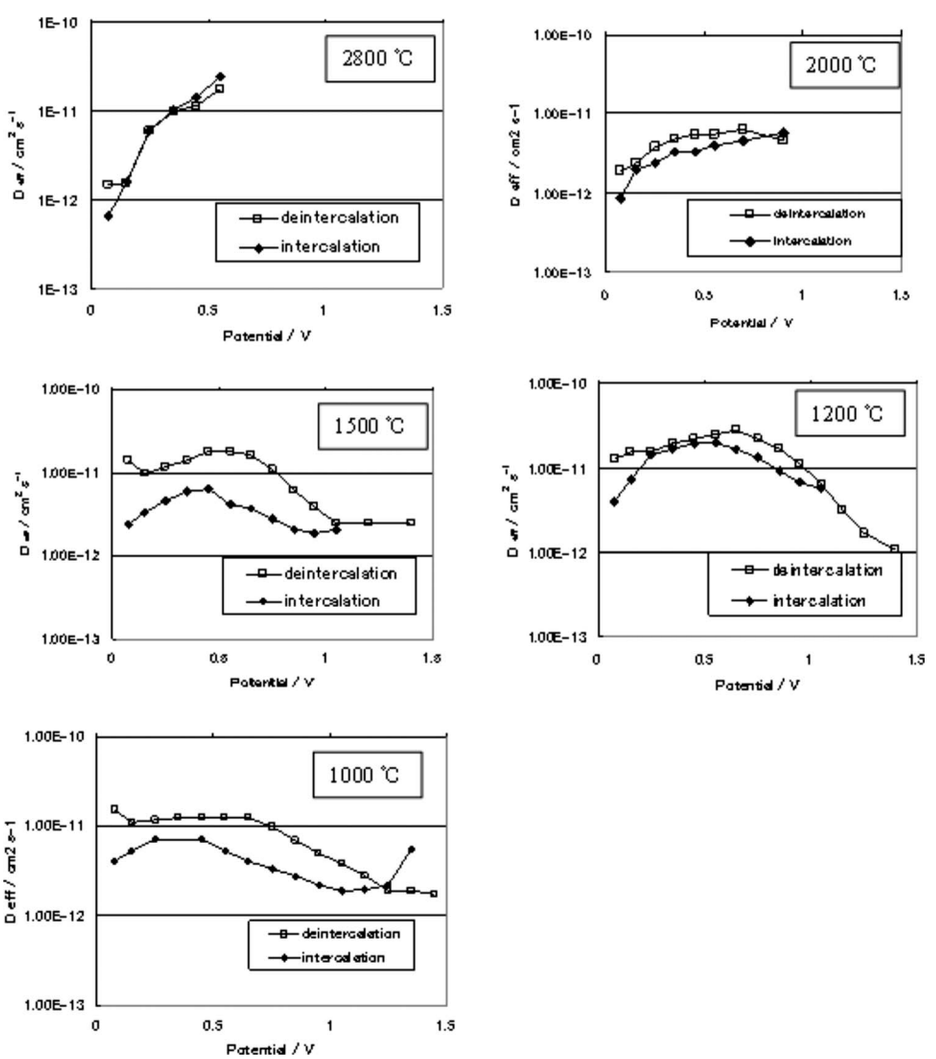

Figure 10. Plots of chemical diffusion coefficients vs potential for CNB.

Comparing 2800 and 2000°C heat-treated CNBs, D_{Li^+} for 2000°C was larger below 0.2 V and smaller above 0.2 V. The D_{Li^+} difference in the direction of intercalation/deintercalation was observed in 1500, 1200, and 1000°C heat-treated CNBs. The difference in direction was not observed at 2800°C. For the 2800°C case, D_{Li^+} is controlled by the lithium-ion diffusion in the CNB. The diffusion coefficient D_{Li^+} does not differ depending on the direction of intercalation/deintercalation[1,17] if the rate-determining step is the lithium-ion diffusion within the CNB. We think that for the 1500, 1200, and 1000°C heat-treated CNBs, control is via interfacial lithium-ion transfer.

Below 1500°C heat-treatments, there are peaks of D_{Li^+} between the 0.3 and 0.7 V range. The D_{Li^+} of the intercalation direction at 1200°C is larger than that for other CNBs. The high value of D_{Li^+} in the 1200°C heat-treated CNB is consistent with the results of CV, charge/discharge, and potential step.

Conclusion

We investigated the electrochemical characteristics of CNB by the microelectrode method. From the results of CV, below 1500°C an anodic current peak was observed at around 1 V and above 2000°C the anodic current peak was below 0.5 V. At a high sweep rate, the capacity in the 2800°C heat-treated CNB and MCMB was much lower than that below 1500°C.

The 1200°C heat-treated CNB showed the highest discharge capacity at a high rate measured by constant current charge/discharge. It was possible to discharge above 1000 C.

The discharge time was measured by the potential step method. The discharge time was longest for the 2800°C heat-treated CNB. The discharge time for MCMB was much shorter than for the 2800°C heat-treated CNB. The charge time was ordered by the temperature of heat-treatment. A higher temperature showed a longer charge time. MCMB was much longer than the 2800°C heat-treated CNB. This result is opposite to discharge.

Lithium-ion diffusion coefficient in CNB was measured by PITT. The 1200°C heat-treated CNB showed the highest current density. In the 2800°C heat-treated CNB, there is little difference in both directions, intercalation/deintercalation, as compared with other temperatures. The intercalation direction dependence was large below the 1500°C heat-treated CNB. The potential of the maximum value of the diffusion coefficient was different for the direction of intercalation/deintercalation.

TDK Corporation assisted in meeting the publication costs of this article.

References

1. M. D. Levi and D. Aurbach, *J. Phys. Chem. B*, **101**, 4641 (1997).
2. M. D. Levi and D. Aurbach, *J. Electroanal. Chem.*, **421**, 79 (1997).
3. M. D. Levi, E. Markevich, and D. Aurbach, *J. Phys. Chem. B*, **109**, 7420 (2005).
4. A. Funabiki, M. Inaba, T. Abe, and Z. Ogumi, *J. Electrochem. Soc.*, **146**, 2443 (1999).
5. A. Funabiki, M. Inaba, T. Abe, and Z. Ogumi, *Electrochim. Acta*, **45**, 865 (1999).
6. B. Markovsky, M. D. Levi, and D. Aurbach, *Electrochim. Acta*, **43**, 2284 (1998).
7. B. Markovsky, M. D. Levi, and D. Aurbach, *Electrochim. Acta*, **43**, 2287 (1998).
8. H. Wang, T. Abe, S. Maruyama, Y. Iriyama, Z. Ogumi, and K. Yoshikawa, *Adv. Mater. (Weinheim, Ger.)*, **17**, 2857 (2005).
9. K. Dokko, M. Mohamedi, Y. Fujita, T. Itoh, M. Nishizawa, M. Umeda, and I. Uchida, *J. Electrochem. Soc.*, **148**, A422 (2001).
10. T. Nishina, H. Ura, and I. Uchida, *J. Electrochem. Soc.*, **144**, 1273 (1997).
11. I. Uchida, H. Fujiyoshi, and S. Waki, *J. Power Sources*, **68**, 139 (1997).
12. Y. Yamamoto, T. Tahara, and R. Harada, Japanese Pat. 2003-1803 (2003).
13. J. R. Dahn, A. K. Sleigh, H. Shi, J. N. Reimers, Q. Zhong, and B. M. Way, *Electrochim. Acta*, **38**, 1179 (1993).
14. E. Buiel and J. R. Dahn, *Electrochim. Acta*, **45**, 121 (1999).
15. T. Zheng, W. R. McKinnon, and J. R. Dahn, *J. Electrochem. Soc.*, **143**, 2137 (1996).
16. K. Tatsumi, T. Akai, T. Imamura, K. Zaghib, N. Iwashita, S. Higuchi, and Y. Sawada, *J. Electrochem. Soc.*, **143**, 1923 (1996).
17. J. S. Gnanaraj, M. D. Levi, E. Levi, G. Salitra, D. Aurbach, J. E. Fischer, and A. Claye, *J. Electrochem. Soc.*, **148**, A525 (2001).
18. C. J. Wen, B. A. Boukamp, R. A. Huggins, and W. Weppner, *J. Electrochem. Soc.*, **126**, 2258 (1979).